

Optical characterization of C O 2 -laser-ablated Si-rich Si O x

Gong-Ru Lin, Chun-Jung Lin, and Yia-Chung Chang

Citation: *Applied Physics Letters* **90**, 151903 (2007); doi: 10.1063/1.2721141

View online: <http://dx.doi.org/10.1063/1.2721141>

View Table of Contents: <http://scitation.aip.org/content/aip/journal/apl/90/15?ver=pdfcov>

Published by the [AIP Publishing](#)

Articles you may be interested in

[Influence of annealing on the Er luminescence in Si-rich SiO₂ layers coimplanted with Er ions](#)

J. Appl. Phys. **104**, 103522 (2008); 10.1063/1.3021414

[Work function thermal stability of Ru O 2 -rich Ru–Si–O p -channel metal-oxide-semiconductor field-effect transistor gate electrodes](#)

J. Appl. Phys. **103**, 073702 (2008); 10.1063/1.2901016

[Residual stress in Si nanocrystals embedded in a Si O 2 matrix](#)

Appl. Phys. Lett. **89**, 053111 (2006); 10.1063/1.2260825

[Electron-beam deposited Si O 2 investigated by scanning capacitance microscopy](#)

Appl. Phys. Lett. **88**, 122116 (2006); 10.1063/1.2189030

[Mechanism of stress relaxation in Ge nanocrystals embedded in Si O 2](#)

Appl. Phys. Lett. **86**, 063107 (2005); 10.1063/1.1856132

The advertisement features a dark blue background with white and orange text. At the top left, it reads 'NEW! Asylum Research MFP-3D Infinity™ AFM' in large white letters, followed by 'Unmatched Performance, Versatility and Support' in orange. To the right is the 'OXFORD INSTRUMENTS' logo in white on a dark blue rectangle, with the tagline 'The Business of Science®' below it. The central part of the ad is divided into four quadrants, each with an image and text: top-left shows a blue textured surface with 'Stunning high performance'; top-right shows a brown textured surface with 'Simpler than ever to GetStarted™'; bottom-left shows a yellow and brown patterned surface with 'Comprehensive tools for nanomechanics'; bottom-right shows a white and blue AFM instrument with 'Widest range of accessories for materials science and bioscience'.

NEW! Asylum Research MFP-3D Infinity™ AFM
Unmatched Performance, Versatility and Support

OXFORD INSTRUMENTS
The Business of Science®

Stunning high performance

Simpler than ever to GetStarted™

Comprehensive tools for nanomechanics

Widest range of accessories for materials science and bioscience

Optical characterization of CO₂-laser-ablated Si-rich SiO_x

Gong-Ru Lin^{a)}

Graduate Institute of Electro-Optical Engineering and Department of Electrical Engineering,
National Taiwan University, No. 1, Sec. 4, Roosevelt Road, Taipei, Taiwan 106, Republic of China

Chun-Jung Lin

Department of Photonics and Institute of Electro-Optical Engineering, National Chiao Tung University,
1001 Ta Hsueh Road, Hsinchu, Taiwan 300, Republic of China

Yia-Chung Chang

Research Center for Applied Sciences, Academia Sinica, 128 Academia Road, Sec. 2, Nankang, Taipei,
Taiwan 115, Republic of China

(Received 28 November 2006; accepted 9 March 2007; published online 9 April 2007)

Anomalous absorption and the corresponding change in the optical band gap of a CO₂-laser-ablated Si-rich SiO₂ (SiO_x) film are studied. The optical band gap energy of as-grown nonstoichiometric SiO_x is slightly reduced by increasing Si–Si bonds as compared to quartz. After rapid thermal annealing using a CO₂ laser, the dehydrogenation of SiO_x film further increases the Si–Si bonding states and redshifts the optical band gap by 1 eV. Laser ablation is initiated at a laser intensity of >7.5 kW/cm², leaving numerous luminescent centers that are related to neutral oxygen vacancy defects, increasing the absorption coefficient and related optical band gap energy, and reducing the refractive index in partially annealed SiO_x. © 2007 American Institute of Physics.

[DOI: 10.1063/1.2721141]

The optical properties of Si-rich SiO₂ (SiO_x) film grown by plasma-enhanced chemical vapor deposition (PECVD) are of great interest because of its extensive applications in Si-based photonics.¹ Self-aggregation of Si nanocrystals (nc-Si) can typically be obtained in SiO_x layer after a high-temperature furnace annealing over 1000 °C. However, the high annealing temperature used to induce the formation of nc-Si may exceed the thermal budget in complementary metal-oxide-semiconductor processes. Since SiO_x exhibits an absorption coefficient of $1.2 \times 10^3 \text{ cm}^{-1}$ at a wavelength of 10.6 μm,² a CO₂ laser annealing technology for synthesizing nc-Si in SiO_x (Refs. 3–5) has recently emerged to overcome the concern about heat-induced damage of nearby integrated circuits. CO₂ laser rapid thermal annealing (RTA) thus provides a convenient approach for the *in situ* precipitation of nc-Si in SiO_x. However, ablation occurs at a laser intensity of >6 kW/cm². The evolution of optical characteristics of the CO₂-laser-ablated SiO_x film is not yet well understood. In this work, an ultraviolet-visible-near infrared (UV-VIS-NIR) transmission/reflection spectroscopic diagnosis is adopted to analyze anomalous absorption spectra, corresponding changes in optical band gap energy, and reciprocal band edge absorption of a CO₂-laser-ablated PECVD-grown SiO_x film. Structural damage induced luminescent centers embedded in CO₂-laser-ablated PECVD-grown SiO_x films were also characterized.

A 280 nm SiO_x film was grown on a 1-mm-thick polished quartz substrate (GE, Type 219). The PECVD was operated at a N₂O/SiH₄ fluence ratio of 6 under an inductively coupling plasma power of 45 W and a chamber pressure of 120 mtorr. The N₂O fluence was maintained at 120 SCCM (SCCM denotes cubic centimeter per minute at STP) during 5 min of growth. The composition of SiO_x was analyzed by

Rutherford backscattering spectrometry, which yielded a calculated O/Si ratio of 1.25 and a total Si concentration of 44.44 at. %. After deposition, a continuous-wave CO₂ laser (LTT Corp., ILS-II) was adopted to perform annealing in ambient atmosphere for 1 ms with intensities from 1.5 to 13.5 kW/cm². Photoluminescence (PL) of the CO₂-laser-treated SiO_{1.25} film was excited by a HeCd laser with a laser intensity (P_{laser}) of 5 W/cm² at 325 nm. The beam spot sizes of the CO₂ laser for RTA and the HeCd laser for PL are about 500 and 30 μm, respectively. The transmittance and reflectance of the SiO_{1.25} films between 190 and 850 nm (with 0.1 nm resolution) were analyzed using a UV-VIS-NIR spectrophotometer (Shimadzu, UV-2401PC).

Several mechanisms related to the redshift in the absorption spectrum of CO₂ laser RTA SiO_{1.25} film are considered, including an increase in the number of Si–Si bonding states, dehydrogenation, precipitation of nc-Si, generation of oxygen-related defects, and variation in the composition of the SiO_{1.25} film. After deposition, a slight redshift of the as-grown SiO_{1.25} at a transmission of 50% increases from 300 to 320 nm in comparison with that of quartz substrate, as shown in the inset of Fig. 1. The absorption peak is at 300 nm with a full width at half maximum of 68 nm, which reveals the decrease in the optical band gap energy of the as-grown SiO_{1.25}. As the mole ratio x decreases from 2.0 to 1.25, the valence and conduction band edges of the SiO_x tailor into its forbidden region; the increased number of Si–Si bonding states is gradually overlaid with the oxygen nonbonding states and finally spread out into the Si valence band. As a result, the band gap energy of the PECVD-grown SiO_x film declines because of the increase in the number of Si–Si bonds in the nonstoichiometric SiO_x, which becomes more significant when nc-Si precipitates in the CO₂ laser RTA SiO_x. Electron-energy-loss spectroscopy also yields evidence of the decrease in the excitation energy of the inner-shell electrons of the Si atom in the CO₂ laser RTA SiO_x. The

^{a)} Author to whom correspondence should be addressed; Fax: +886-2-33669598; electronic mail: grlin@ntu.edu.tw

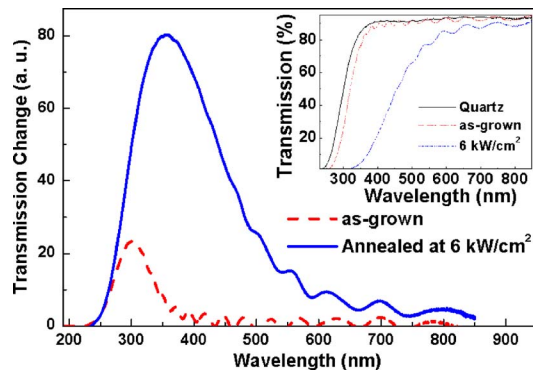


FIG. 1. (Color online) Transmission change of as-grown $\text{SiO}_{1.25}$ and CO_2 laser annealed $\text{SiO}_{1.25}$ at $P_{\text{laser}}=6 \text{ kW/cm}^2$. Inset: Transmission spectra of pure quartz, as-grown $\text{SiO}_{1.25}$, and CO_2 laser annealed $\text{SiO}_{1.25}$ at $P_{\text{laser}}=6 \text{ kW/cm}^2$.

modification on the absorption band edge as well as the optical band gap by detuning stoichiometry during growth or by self-assembling Si nanocrystals after CO_2 laser RTA was thus confirmed. Therefore, the slight redshift in the transmission of as-grown $\text{SiO}_{1.25}$ in comparison with that of quartz substrate is caused by the increasing number of Si-Si bonds in $\text{SiO}_{1.25}$ near the valence and conduction band edges.

The wavelength of 50% transmission of annealed $\text{SiO}_{1.25}$ after CO_2 laser RTA at $P_{\text{laser}}=6 \text{ kW/cm}^2$ is greatly increased from 320 to 457 nm in comparison with that of as-grown $\text{SiO}_{1.25}$. The peak of the change in the transmission of the annealed sample is significantly redshifted from 300 to 356 nm, associated with an increase in the peak absorption by a factor of 4, as presented in Fig. 1. At a CO_2 laser RTA intensity below the ablation threshold, the effect of increasing Si-Si bonding states on the clearly tuned blue-green absorption edge is thus stronger than any other effect. The near-band-edge absorption coefficient is further understood by decomposing the absorption coefficient (α) from the transmission and reflection spectra according to the following equation:⁶

$$\alpha = -\frac{1}{d} \ln \left(\frac{\sqrt{(1-R)^4 + 4T^2R^2} - (1-R)^2}{2TR^2} \right), \quad (1)$$

where d is the thickness of the film, T is the transmission, and R is the reflectance. CO_2 laser RTA at 6 kW/cm^2 caused a redshift of nearly 1 eV on the absorption band edge of the $\text{SiO}_{1.25}$ (see Fig. 2). Since the reactants are SiH_4 and N_2O , the as-PECVD-grown $\text{SiO}_{1.25}$ film contains a high concentra-

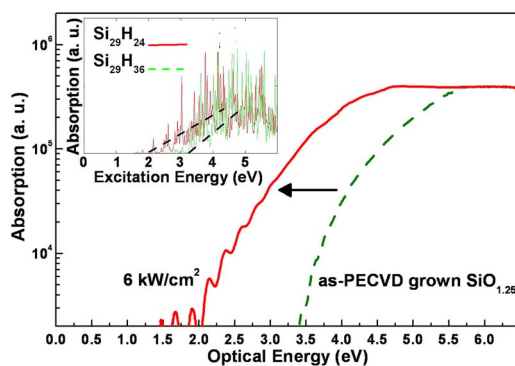


FIG. 2. (Color online) Absorption spectra of as-grown $\text{SiO}_{1.25}$ and CO_2 laser annealed $\text{SiO}_{1.25}$ at $P_{\text{laser}}=6 \text{ kW/cm}^2$. Inset: The calculated absorption spectra of $\text{Si}_{29}\text{H}_{24}$ and $\text{Si}_{29}\text{H}_{36}$.

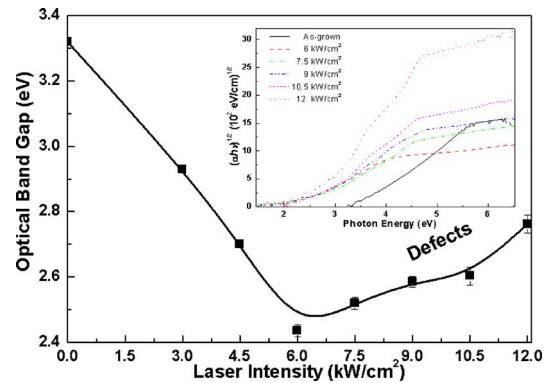


FIG. 3. (Color online) Optical band gap of CO_2 laser annealed $\text{SiO}_{1.25}$ as a function of laser intensity. Inset: Tauc plot, $(\alpha h\nu)^{1/2}$ as a function of photon energy ($h\nu$) for as-grown $\text{SiO}_{1.25}$ sample and CO_2 laser RTA $\text{SiO}_{1.25}$ samples at P_{laser} from 6 to 12 kW/cm^2 .

tion of hydrogen. Hydrogen passivation can be released from $\text{SiO}_{1.25}$ during CO_2 laser annealing. The loss of hydrogen causes compaction of $\text{SiO}_{1.25}$, a decrease in the thickness of $\text{SiO}_{1.25}$ during annealing, and a variation in the composition of $\text{SiO}_{1.25}$ film. The absorption spectra of hydrogen-passivated Si clusters were calculated by solving the many-body Bethe-Salpeter equation⁷ with a symmetrized plane wave basis, while the *ab initio* nonseparable pseudopotential code that was based on the linear augmented Slater-type orbital (LASTO by Brookhaven National Laboratory) model⁸ was adopted to accelerate computation efficiency. The calculated absorption band edge was also redshifted by almost 1 eV as the number of surrounding hydrogen atoms decreased from 36 to 24. Dehydrogenation not only reduces the thickness of the PECVD-grown SiO_x film but also increases the number of Si-Si bonding states, contributing to the redshift of the optical band gap. Figure 3 plots the evolution on the optical band gap energy of the $\text{SiO}_{1.25}$ with increasing CO_2 laser RTA intensity, which is mainly attributed to non-stoichiometric growth, dehydrogenation, and Si precipitation in PECVD-grown $\text{SiO}_{1.25}$ under the ablation threshold. The slope of the laser-intensity-dependent change in the optical band gap is $-0.148 \text{ eV/kW/cm}^2$.

In contrast, the optical band gap energy of the PECVD-grown $\text{SiO}_{1.25}$ increases from 2.43 to 2.76 eV at a CO_2 laser RTA intensity of $>6 \text{ kW/cm}^2$ (see Fig. 3), because the structural defects were generated under high-power CO_2 laser RTA induced ablation. Such CO_2 laser ablation at P_{laser}

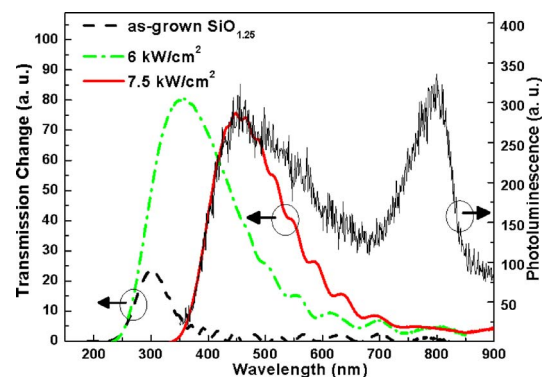


FIG. 4. (Color online) PL spectrum of PECVD-grown $\text{SiO}_{1.25}$ annealed at $\text{CO}_2 P_{\text{laser}}$ of 7.5 kW/cm^2 and transmission change of as-grown $\text{SiO}_{1.25}$ and CO_2 laser annealed $\text{SiO}_{1.25}$ at P_{laser} of 6 and 7.5 kW/cm^2 .

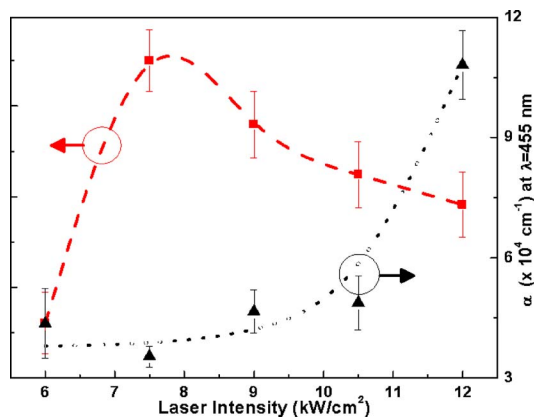


FIG. 5. (Color online) Refractive index and absorption coefficient of CO₂ laser RTA SiO_{1.25} as a function of laser intensity.

>7.5 kW/cm² not only sputters the SiO_{1.25} film out of the substrate but also damages the surface structure without any regrowth. Therefore, the oxygen-defect-related PL at 455 nm is inevitably increased, as shown in Fig. 4. The SiO_{1.25} matrix is rapidly compressed during such rapid laser ablation, where numerous oxygen-dependent defects such as weak oxygen bond,⁹ neutral oxygen vacancy (NOV),¹⁰ and ionized oxygen (O₂⁻) (Ref. 11) with PL wavelengths at 410–455 nm are generated by the damaged bonds of the SiO₂ matrix. The NOV defect may have an important role in the anomalous absorption because the PECVD-grown SiO_{1.25} matrix is originally in an oxygen-deficient environment. Obviously, the adsorption rate of O ions will be much smaller than that of Si ions at a high-temperature and in an oxygen-deficient environment provided by the CO₂ laser RTA of the SiO_{1.25} in ambient atmosphere. Such a phenomenon has never been observed on a SiO_x film that was entirely annealed in a furnace under similar conditions, as furnace annealing usually causes a gradual but complete recovery on the compressing strain of the SiO₂ matrix close to nc-Si. Notably, the transmission change profile of the CO₂-laser-ablated SiO_{1.25} at $P_{\text{laser}} > 7.5$ kW/cm² is highly consistent with the NOV-defect-related blue-green PL spectrum at a peak wavelength of 450–455 nm (see Fig. 4). Such a blue-green PL spectrum has never been observed in the CO₂ laser annealed SiO_{1.25} at <6 kW/cm², which result clearly confirms the contribution of NOV defects generated during CO₂ laser ablation. Additionally, the absorption coefficient of the SiO_{1.25} film at a wavelength of 455 nm increases by three times as the CO₂ laser intensity enlarges from 7.5 to 12 kW/cm² (see Fig. 5). This result again verifies the contribution of ablation-induced surface damage and structural defects at higher laser intensities. The incompletely annealed SiO_{1.25} with many oxygen-dependent defects also suffers from a slight decrease in the refractive indices from 1.87 to 1.79 as P_{laser} increases from 7.5 to 12 kW/cm². In Fig. 5, the threshold CO₂ laser inten-

sity required to initiate the ablation of the SiO_{1.25} film can be clearly obtained from the evolution of both the refractive index and the absorption coefficient.

In conclusion, the anomalous absorption spectra and corresponding changes in optical band gap energy, band edge absorption, and structurally damaged related luminescent centers of the CO₂-laser-ablated PECVD-grown SiO_{1.25} film were characterized using UV-VIS-NIR transmission/reflection and PL spectroscopies. After PECVD deposition, a slight redshift in the transmission and the lower optical band gap energy of as-grown SiO_{1.25} in comparison with those of quartz substrate are due to the increase in the Si–Si bonding state in SiO_{1.25} near the valence and conduction band edges. Since the as-grown SiO_{1.25} film contains a high concentration of hydrogen, dehydrogenation not only reduces the thickness of the PECVD-grown SiO_{1.25} film but also enhances the number of Si–Si bonding states under CO₂ laser RTA below the ablation threshold (6 kW/cm²), hence contributing to a redshift of the optical band gap from 3.32 to 2.43 eV. As the CO₂ laser RTA intensity increases to >6 kW/cm², the optical band gap energy of the PECVD-grown SiO_{1.25} increases oppositely from 2.43 to 2.76 eV due to the ablation-induced damage to the surface and the generated NOV defects. The absorption coefficient of the SiO_{1.25} film at a wavelength of 455 nm is increased by a factor of 3 as the CO₂ laser intensity is increased from 7.5 to 12 kW/cm². During ablation, the incompletely annealed SiO_{1.25} with numerous oxygen-dependent defects also suffers from a slight decrease in the refractive indices from 1.87 to 1.79 when P_{laser} increases from 7.5 to 12 kW/cm².

This work was supported in part by the National Science Council (NSC) of the Republic of China under Grant Nos. NSC95-2221-E-002-448 and NSC95-2120-M-009-006.

- ¹L. Pavesi, L. Dal Negro, C. Mazzoleni, G. Franzò, and F. Priolo, *Nature* (London) **408**, 440 (2000).
- ²E. D. Palik, *Handbook of Optical Constants of Solids* (Academic, New York, 1985), Vol. 1, p. 762.
- ³C. J. Lin, G.-R. Lin, Y. L. Chueh, and L. J. Chou, *Electrochem. Solid-State Lett.* **8**, D43 (2005).
- ⁴G.-R. Lin, C. J. Lin, L. J. Chou, and Y. L. Chueh, *IEEE Trans. Nanotechnol.* **5**, 511 (2006).
- ⁵A. Tewary, R. D. Kekatpure, and M. L. Brongersma, *Appl. Phys. Lett.* **88**, 093114 (2006).
- ⁶D. K. Schroder, *Semiconductor Material and Device Characterization* (Wiley, New York, 1998), Vol. 2, p. 597.
- ⁷V. Garbuio, M. Cascella, L. Reining, R. Del Sole, and O. Pulci, *Phys. Rev. Lett.* **97**, 137402 (2006).
- ⁸Y.-C. Chang, R. B. James, and J. W. Davenport, *Phys. Rev. B* **73**, 035211 (2006).
- ⁹J. C. Cheang-Wong, A. Oliver, J. Roiz, and J. M. Hernandez, *Nucl. Instrum. Methods Phys. Res. B* **175**, 490 (2001).
- ¹⁰G.-R. Lin, C. J. Lin, and K. C. Yu, *J. Appl. Phys.* **96**, 3025 (2004).
- ¹¹C. Itoh, T. Suzuki, and N. Itoh, *Phys. Rev. B* **41**, 3794 (1990).